

# Identification of $\beta$ -hydroxy fatty acid esters and primary, secondary-alkanediol esters in cuticular waxes of the moss *Funaria hygrometrica*

Lucas Busta<sup>a</sup>, Jessica M. Budke<sup>b</sup>, Reinhard Jetter<sup>a,c,\*</sup>

<sup>a</sup> Department of Chemistry, University of British Columbia, 2036 Main Mall, Vancouver, BC V6T 1Z1, Canada

<sup>b</sup> Department of Plant Biology, University of California – Davis, One Shields Ave., Davis, CA 95616, USA

<sup>c</sup> Department of Botany, University of British Columbia, 6270 University Boulevard, Vancouver, BC V6T 1Z4, Canada

## ARTICLE INFO

### Article history:

Received 11 June 2015

Received in revised form 8 October 2015

Accepted 27 October 2015

Available online 6 November 2015

### Keywords:

*Funaria hygrometrica*

Bryophyta

Structure elucidation

Esters

Gametophyte

Sporophyte

Calyptra

Cuticular wax

Very-long-chain

## ABSTRACT

The plant cuticle, a multi-layered membrane that covers plant aerial surfaces to prevent desiccation, consists of the structural polymer cutin and surface-sealing waxes. Cuticular waxes are complex mixtures of ubiquitous, typically monofunctional fatty acid derivatives and taxon-specific, frequently bifunctional specialty compounds. To further our understanding of the chemical diversity of specialty compounds, the waxes on the aerial structures of the leafy gametophyte, sporophyte capsule, and calyptra of the moss *Funaria hygrometrica* were surveyed. Respective moss surfaces were extracted, and resulting lipid mixtures were analyzed by gas chromatography–mass spectrometry (GC–MS). The extracts contained ubiquitous wax compound classes along with two prominent, unidentified classes of compounds that exhibited some characteristics of bifunctional structures. Microscale transformations led to derivatives with characteristic MS fragmentation patterns suggesting possible structures for these compounds. To confirm the tentative structure assignments, one compound in each of the suspected homologous series was synthesized. Based on GC–MS comparison with the authentic standards, the first series of compounds was identified as containing esters formed by  $\beta$ -hydroxy fatty acids and wax alcohols, with ester chain lengths varying from C<sub>42</sub> to C<sub>50</sub> and the most prominent homolog being C<sub>46</sub>. The second series consisted of fatty acid esters of 1,7-alkanediols, linked via the primary hydroxyl group, with ester chain lengths C<sub>40</sub>–C<sub>52</sub> also dominated by the C<sub>46</sub> homolog. The  $\beta$ -hydroxy acid esters were restricted to the sporophyte capsule, and the diol esters to the leafy gametophyte and calyptra. Based on their homolog and isomer distributions, and the presence of free 1,7-triacontanediol, possible biosynthetic reactions leading to these compounds are discussed.

© 2015 Elsevier Ltd. All rights reserved.

## 1. Introduction

The evolutionary transition of plant life from aquatic to terrestrial environments presented great challenges, desiccation being principal among them. One structural feature that helps plants reduce transpiration across their vast aerial surfaces is the cuticle, an extra-cellular membrane covering epidermal cells (Yeats and Rose, 2013). Plant cuticles consist of the fatty acid polyester cutin that provides a structural framework, and embedded waxes that seal the surface (Dominguez et al., 2011). Plant cuticular waxes are complex mixtures of very-long-chain (VLC) fatty acid (FA) derivatives that can be divided into two categories: those that

occur ubiquitously in the wax of almost all plant species, and specialty compounds that are encountered only in the wax of certain plant taxa (Jetter et al., 2006). The ubiquitous wax constituents are mostly VLC aliphatics with one terminal functional group such as fatty acids, aldehydes, and primary alcohols, but may also include alkanes (no functional groups) or dimers formed by ester linkages between fatty acids and wax alcohols (Samuels et al., 2008). Specialty wax compounds are mostly also fatty acid-derived, but may contain more than one functional group including in-chain functionalities, thus creating much greater structural diversity.

Our current understanding of wax biosynthesis is primarily based on molecular genetic and biochemical characterization of model plants, most prominently *Arabidopsis thaliana*, the wax mixtures of which comprise mostly ubiquitously occurring compounds (Jenks et al., 1995; Rashotte et al., 2001). In the wax biosynthetic pathways leading to these wax constituents, two stages can be

\* Corresponding author at: Department of Botany, University of British Columbia, 6270 University Boulevard, Vancouver, BC V6T 1Z4, Canada.

E-mail address: [jetter@mail.ubc.ca](mailto:jetter@mail.ubc.ca) (R. Jetter).

distinguished: elongation and diversification. First, even-carbon-numbered long-chain fatty acyl-CoAs originating from plastidial FA *de novo* biosynthesis are elongated by the addition of C<sub>2</sub> units derived from malonyl-CoA. The fatty acid elongase (FAE) multi-enzyme complex accomplishes the transformation by catalyzing four sequential reactions. Initially a ketoacyl-CoA synthase (KCS) condenses the fatty acyl-CoA and malonyl-CoA substrates to form a  $\beta$ -ketoacyl intermediate (Joubès et al., 2008), then a ketoacyl reductase (KCR) reduces the secondary oxo group to a hydroxyl function (Beaudoin et al., 2009). Next, the  $\beta$ -hydroxyl group is eliminated by a dehydratase (HCD), and the resulting  $\alpha$ ,  $\beta$ -double bond is finally saturated by an enoyl-CoA reductase (ECR) to form a fatty acyl-CoA two carbons longer than the original KCS substrate (Bach et al., 2008; Zheng et al., 2005). Repeated FAE cycles lead to acyl-CoAs with chain lengths typically ranging from C<sub>24</sub> to C<sub>34</sub>.

In the second stage of ubiquitous wax compound biosynthesis, elongated VLC acyl-CoAs are diversified into various derivatives through head group modifications. These take place in a chain-length-specific manner such that the full range or only a selection of the chain lengths in the acyl-CoA precursor pool is found in each of the final wax products. Matching chain length profiles have been reported for the free and esterified *n*-alkanols in various plant species (Lai et al., 2007; Razeq et al., 2014), indicating that the esters and free alkanols are biosynthetically related. Indeed, it has been shown that in *Arabidopsis* a fatty acyl-CoA reductase (FAR) generates VLC *n*-alkanols that are then linked with fatty acyl-CoAs by a wax ester synthase (Li et al., 2008), and that both the alcohol intermediates and the alkyl ester end products are exported to the cuticle. Further chain length comparisons across species suggested that a separate biosynthetic pathway leads to aldehydes and alkanes. Molecular genetic evidence, again for *Arabidopsis*, has confirmed that reduction of VLC acyl-CoAs truly leads to even-carbon-numbered aldehydes and further decarbonylation to corresponding odd-carbon-numbered alkanes (Bernard et al., 2012; Chen et al., 2003).

While the biosynthesis of the ubiquitous wax compounds is well understood, the processes leading to specialty compounds have received far less attention. Exceptions to this are the secondary alcohols, diols, ketones, and ketols found as major constituents of Brassicaceae waxes (Lee et al., 2015; Zhang et al., 2013). Again, homolog profiles suggest a biosynthetic relationship: that all these specialty compound classes are derived from the ubiquitous alkanes. Further detailed isomer analysis of *Arabidopsis* stem wax constituents with secondary functional groups indicates that hydroxylation on one or more of three carbon atoms near the center of alkane precursor molecules likely leads to the secondary alcohols, and repeat hydroxylation or oxidation to the ketones, diols, and ketols (Wen and Jetter, 2009). Molecular genetic investigations confirmed this hypothesis, and a P450 monooxygenase with mid-chain alkane hydroxylase (MAH) activity was shown to be involved in the process by oxidizing any carbon from C-13 to C-15 of the C<sub>29</sub> alkane chain to produce a mixture of isomers whose secondary functional groups are on adjacent carbons (Greer et al., 2007).

Many other wax compounds with one or more secondary oxygen-containing functional groups that do not seem to be biosynthetically related to the secondary functional compounds of the Brassicaceae have been described as major wax constituents in several plant taxa. For example, the secondary alcohol 10-nonacosanol is a very prominent wax component of various gymnosperm and angiosperm taxa, as well as multiple *Pogonatum* moss species (Barthlott et al., 1996; Jetter et al., 1996; Neinhuis and Jetter, 1995). In contrast to the isomer mixtures of *Arabidopsis* secondary alcohols, this compound usually appears as a single isomer, and while some species also contained trace amounts of 8- or 12-nonacosanol, the 9- or 11-isomers were not detected. Similarly, ketones have been found in some plant waxes, most prominently

on the fern *Osmunda regalis* (Jetter and Riederer, 2000), and also in the form of  $\beta$ -diketones in the Poaceae (Barthlott et al., 1998). Based on their isomer patterns, these wax constituents with secondary functionalities have long been suspected to originate from processes other than P450 hydroxylation, possibly through the activity of polyketide synthase (PKS) enzymes (von Wettstein-Knowles, 1995). In essence, their secondary functional groups were hypothesized to originate during chain elongation, as remnants of  $\beta$ -functionalities introduced through Claisen condensation reactions, thus explaining their exclusive presence on particular carbons. Diverse biochemical experiments have since confirmed this hypothesis for  $\beta$ -diketones, but have not provided information about the enzymes and genes involved (von Wettstein-Knowles, 1993). Similar biochemical and molecular genetic evidence is also lacking for other specialty compounds.

In the absence of enzymological or genetic information, the biosynthetic machinery behind the formation of specialty wax constituents is best assessed by further detailed analyses of diverse compounds with secondary functionalities. In particular, those with oxygen functionalities on both a primary and a secondary carbon are informative, for example 5-hydroxy aldehydes and 1,5-alkanediols in *Taxus baccata* and 5-hydroxy acids in *Cerintho minor* (Jetter and Riederer, 1999a; Wen and Jetter, 2007), 11-keto alcohols and aldehydes in *O. regalis* (Jetter and Riederer, 1999b), 1,7-, 1,9-, and 1,11-diols in *Papaver alpinum* (Jetter et al., 1996), and 3-hydroxy fatty acids in *Aloe arborescens* (Racovita et al., 2014). The primary functionalities therein added substantial chemical diversity in the form of compound classes with terminal carboxylic acid, ester, aldehyde, or alcohol group. Comparisons between the homolog and isomer patterns of these bifunctional compound classes, where they were co-occurring, thus proved to be particularly informative for narrowing down possible, novel biosynthetic pathways.

In order to further our understanding of wax biosynthesis, novel compounds with both primary and secondary functional groups have to be identified, which necessitates analyses of waxes from diverse plant lineages. It is important that both vascular and non-vascular plants are included in this survey, especially since specialty compounds have been found as prominent members of the waxes of angiosperms, gymnosperms, ferns, and mosses alike. Most notably, waxes from several Polytrichales mosses comprised large percentages of compounds with secondary functional groups, including 10-nonacosanol (Neinhuis and Jetter, 1995). Waxes of *Andreaea*, *Pogonatum*, *Syntrichia*, and *Physcomitrella* moss species contained ubiquitous wax compounds including fatty acids, alkanols, alkyl esters, aldehydes, and alkanes (Buda et al., 2013; Haas, 1982; Xu et al., 2009). However, bifunctional compound classes from moss waxes have yet to be identified. The goal of the present study was to provide further moss wax analyses and to identify bifunctional compounds if possible.

Recently, microscopic examination of multiple structures of the moss *Funaria hygrometrica* revealed that the calyptra, a maternal protective structure of mosses, has a cuticle (Budke et al., 2011). Interest in the wax of a cuticle that had not been previously analyzed prompted a preliminary analysis, which indicated the presence of unknown compounds that potentially contained two functional groups. As candidates for compounds that could expand our understanding of the diversity and potentially the biosynthesis of specialty wax compounds, structural elucidation of these compounds was the focus of this work. Accordingly, waxes were extracted from the surfaces of the three main structures of *F. hygrometrica*, the maternal leafy gametophyte, the offspring sporophyte capsule, and the maternal calyptra. The wax mixtures were separated with thin layer chromatography (TLC) where necessary, and analyzed as trimethylsilyl (TMS) derivatives with GC-MS. Authentic standards were then synthesized to confirm the structures of the unknown compounds.

## 2. Results

The aim of the present work was to identify novel compounds in the cuticular waxes covering various *F. hygrometrica* structures. Extracts from the surfaces of the calyptra, leafy gametophyte, and sporophyte capsule yielded typical wax mixtures composed of VLC fatty acids, *n*-alkanols, alkyl esters, aldehydes, and alkanes, together with two prominent groups of novel compounds. One was found in the calyptra and leafy gametophyte waxes (designated compound class **A**), and the other in the sporophyte capsule samples (compound class **B**). Mass spectroscopic analysis and organic synthesis were used to determine the structures of the compounds in each group.

### 2.1. Identification and relative quantification of compounds in series **A**

To isolate compound class **A**, surface wax was extracted from several hundred leafy gametophytes and separated into three fractions using TLC. An aliquot of each fraction was reacted with bis-*N*, *O*-(trimethylsilyl)-trifluoroacetamide (BSTFA) to form TMS derivatives of groups with exchangeable protons, and the resulting mixtures were analyzed with GC–MS. Compound class **A** was found in a fraction ( $R_f$  0.39) well separated from all other wax components and running between *n*-alcohols and wax esters. Initial GC–MS analysis indicated that fraction **A** contained seven compounds (Fig. 1A) that shared MS characteristics. Their fragmentation patterns included some fingerprint ions that were identical between all seven compounds and some with differences of  $m/z$  28 between them. Based on this MS behavior and the evenly spaced GC peaks, fraction **A** was recognized as a series of seven homologous compounds.

All members of unknown series **A** had high GC retention times and contained fragments larger than  $m/z$  700+ in their mass spectra, both reminiscent of alkyl esters formed by monofunctional wax alcohols and acids. To assess whether fraction **A** contained similar ester-linked dimers, and to determine the number and nature of the functional groups involved, the remainder of the TLC fraction was subjected to transesterification with  $\text{BF}_3$  and methanol followed by TMS derivatization. GC–MS analysis showed that the reaction mixture contained eight major compounds, which were identified as the methyl ester TMS ether derivatives of  $\text{C}_{20}$ ,  $\text{C}_{22}$ ,  $\text{C}_{24}$ , and  $\text{C}_{26}$   $\beta$ -hydroxy fatty acids, and as TMS ethers of  $\text{C}_{20}$ ,  $\text{C}_{22}$ ,  $\text{C}_{24}$ , and  $\text{C}_{26}$  *n*-alkanols. The  $\text{C}_{24}$   $\beta$ -hydroxy fatty acid methyl ester and  $\text{C}_{22}$  *n*-alkanol were found to predominate (Fig. S1). Thus, the initial analysis suggested that the compounds in series **A** were VLC  $\beta$ -hydroxy fatty acid alkyl esters.

Next, the mass spectra of the TMS derivatives of the compounds in **A** were examined to further confirm their potential  $\beta$ -hydroxy fatty acid ester structures. All seven spectra exhibited (i) prominent fragments  $m/z$  73  $[\text{Si}(\text{CH}_3)_3]^+$  indicative of a TMS-derivatized hydroxyl group, (ii) series of fragments  $m/z$  57, 71, 85, 99, etc.  $[(\text{C}_n\text{H}_{n+1})^+]$  suggesting at least one aliphatic tail, and (iii) fragments  $m/z$  145 and 161, likely due to combined  $\alpha$ -fragmentation and rearrangement, indicating a  $\beta$ -hydroxy acid moiety (Fig. S2).

Each of the seven mass spectra exhibited further characteristic fragments, including ions  $[\text{M}-15]^+$ , possibly due to methyl loss, and  $[\text{M}-90]^+$ , potentially due to  $\text{HOSi}(\text{CH}_3)_3$  elimination from the parent molecules ( $m/z$  750 and 675, respectively, for the  $\text{C}_{46}$  compound in Fig. 1C)<sup>1</sup>. These fragments differed by  $m/z$  28 between

homologs. A third fragment, likely arising from McLafferty rearrangement with double hydrogen transfer ( $r_2\text{H}$ , Fig. 1E), was observed as a small peak in each spectrum ( $m/z$  457 for the  $\text{C}_{46}$  compound). Finally, two  $\alpha$ -fragments generated about either side of the (TMS-derivatized) hydroxyl group indicated the presence of one alkyl tail and a carboxyl head group ( $m/z$  397 and 469 for the  $\text{C}_{46}$  compound), which confirmed the  $\beta$ -hydroxy acid ester structure. The major isomer of the  $\text{C}_{46}$  compound was thus tentatively identified as the  $\text{C}_{22}$  alkyl ester of  $\text{C}_{24}$   $\beta$ -hydroxy acid (docosyl 3-hydroxytetracosanoate).

It should be noted that the  $\alpha$ -fragments of the  $\beta$ -hydroxyl function were flanked by pairs of homologous ions ( $m/z$  369 and 497, as well as  $m/z$  341 and 525 for the  $\text{C}_{46}$  ester, Fig. S2), suggesting the presence of isomeric  $\beta$ -hydroxy acid esters with shorter alcohol and correspondingly longer  $\beta$ -hydroxy acid moieties. The presence of such ester isomers was confirmed by corresponding rearrangement fragments ( $m/z$  385, 413, 441 for the  $\text{C}_{46}$  homolog, Fig. S2), present in approximately the same ratios as the parent ions. The relative abundances of these ions did not vary within individual ester homolog peaks, indicating that the ester isomers were not GC-separated under our conditions.

To confirm the structure assignment for fraction **A**, an authentic standard of docosyl 3-hydroxytetracosanoate was synthesized (Fig. 2). To this end, docosanol (**1**) was transformed into both docosyl 2-bromoacetate (**2**) and docosanal (**3**) via reaction with bromoacetyl chloride and oxidation with anhydrous PCC, respectively. Mass spectroscopic characterization of these intermediates is provided in the Supplementary data (Figs. S3 and S4). A Reformatsky reaction was then used to unite **2** and **3** to obtain docosyl 3-hydroxytetracosanoate (**4**). The final product was isolated by preparative TLC and found to co-migrate on analytical TLC with the natural product. A TMS derivative of the TLC-purified synthetic standard had mass spectroscopic and GC retention behavior identical to those of one isomer of one homolog in series **A**, thus confirming the identity of the latter. Examining all the evidence jointly, the compounds in fraction **A** were identified as homologous  $\beta$ -hydroxy fatty acid esters of the four even- and three odd-numbered chain lengths ranging from  $\text{C}_{42}$  to  $\text{C}_{48}$  (Fig. 1A–D).

The relative amounts of the hydroxyester homologs were quantified in the wax mixtures from different moss organs by integrating appropriate selected ion chromatograms ( $m/z$  161). In the calyptra wax, the seven  $\beta$ -hydroxy fatty acid esters with even-numbered chain lengths between  $\text{C}_{40}$  and  $\text{C}_{52}$  were found in a bimodal distribution with peaks at  $\text{C}_{42}$  and  $\text{C}_{50}$  (Fig. 3). In the total wax mixture from leafy gametophytes, 13  $\beta$ -hydroxy fatty acid ester homologs ranging from  $\text{C}_{40}$  to  $\text{C}_{52}$  were detected, thus even more than in the corresponding TLC fraction (Fig. 1A). The distribution of these compounds in the leafy gametophyte wax was approximately normal with a peak at  $\text{C}_{46}$ .

### 2.2. Identification and relative quantification of compound class **B**

The next objective was to identify the constituents of compound class **B**. Since relatively little sporophyte capsule wax was available, the structure elucidation had to be carried out directly from the total wax mixture without prior TLC separation. However, the TMS derivatives of series **B** obtained without pre-separation proved to have MS characteristics that enabled a tentative structure assignment. Late-eluting, regularly spaced GC peaks (Fig. 4A) and multiple homologous MS fragments again indicated that all compounds in **B** belonged to one homologous series.

The mass spectra of the TMS derivatives of all homologs in series **B** had four characteristics in common (Fig. 3C): (i) prominent

<sup>1</sup> Due to the high number of carbon atoms in wax molecules and thus the high probability of  $^{13}\text{C}$  and  $^2\text{D}$  incorporation, large fragments such as  $[\text{C}_n\text{H}_{2n+1}\text{OTMS}-15]^+$  are expected to have average  $m/z$  ( $3n \cdot 0.01$ ) units more than the nominal mass. The standard resolution of the MS data acquisition system used here rounds  $m/z$  values to the nearest integer and will thus report  $m/z$  750 for the above ion.

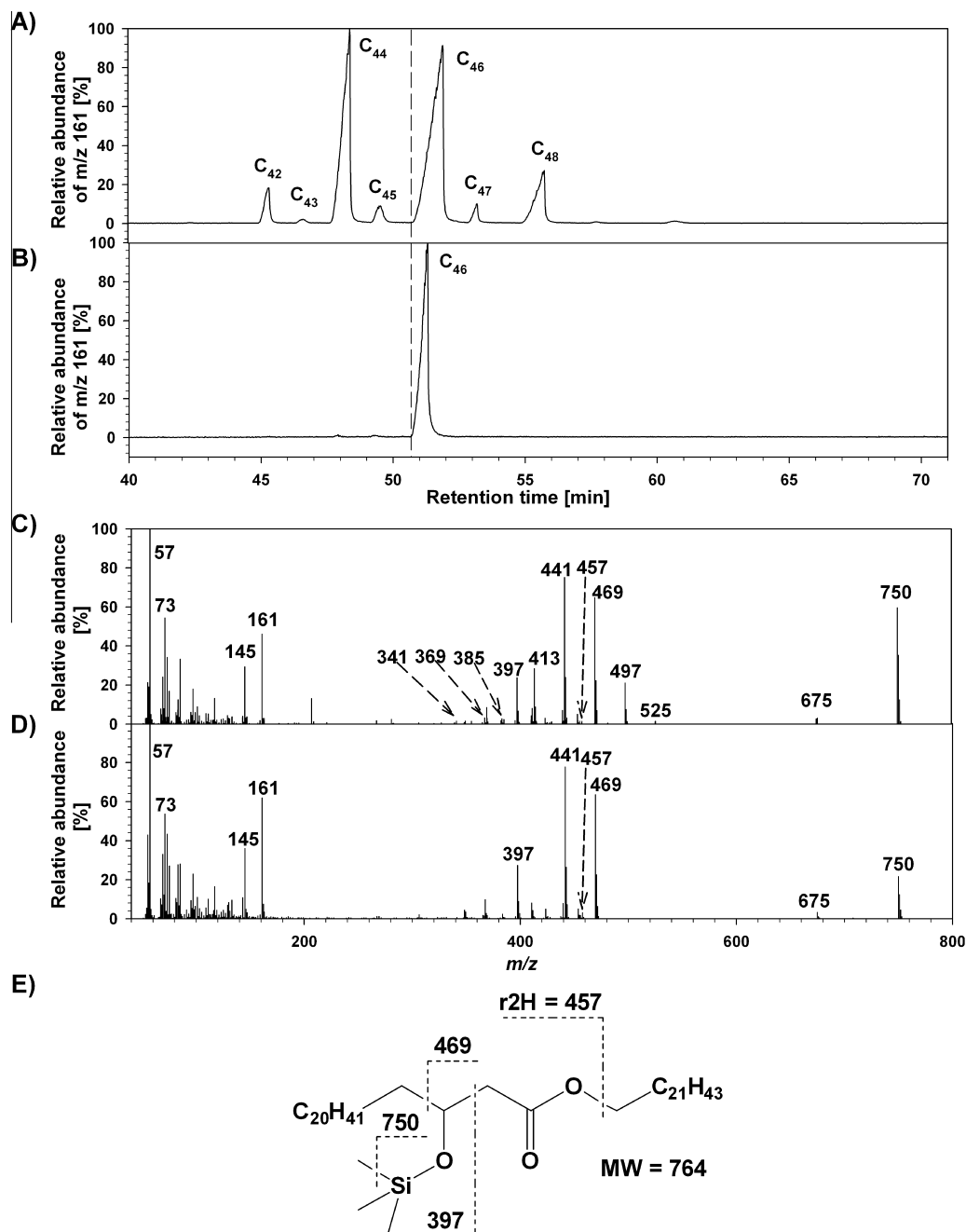


**Fig. 1.** Identification of unknown series **A** found in *Funaria hygrometrica* calyptra and leafy gametophyte waxes. (A) Selected ion chromatogram ( $m/z$  161) of fraction **A** isolated from the leafy gametophyte extract using TLC. (B) Selected ion chromatogram ( $m/z$  161) of synthetic  $C_{46}$   $\beta$ -hydroxy fatty acid ester (docosyl 3-hydroxytetracosanoate (**4**), obtained from docosanol (**1**), see Fig. 2). (C) EI mass spectrum of the most abundant homolog ( $C_{46}$ ) in (A). (D) EI mass spectrum of the synthetic  $C_{46}$   $\beta$ -hydroxy fatty acid ester shown in (B). (E) Potential routes to the major fragments observed in the mass spectra of the  $C_{46}$   $\beta$ -hydroxy fatty acid ester. Additional fragmentation mechanisms and ions resulting from the fragmentation of other  $C_{46}$   $\beta$ -hydroxy acid isomers are described in Fig. S5.

fragments  $m/z$  73 ( $[\text{Si}(\text{CH}_3)_3]^+$ ), but not  $m/z$  147 ( $[(\text{CH}_3)_3\text{SiOSi}(\text{CH}_3)_2]^+$ ), indicating the presence of only one hydroxyl functionality, (ii) alkyl fragments  $m/z$  57, 71, etc.  $[\text{C}_n\text{H}_{2n+1}]^+$ , suggesting the presence of at least one unfunctionalized hydrocarbon terminus, (iii) a pair of fragments  $m/z$  239 and 257 interpreted as  $[\text{CH}_3(\text{CH}_2)_{14}\text{CO}]^+$  and  $[\text{CH}_3(\text{CH}_2)_{14}\text{C}(\text{OH})_2]^+$ , respectively, and hence pointing to the presence of a  $C_{16}$  acid moiety, and (iv) a pair of fragments  $m/z$  313 ( $[\text{CH}_3(\text{CH}_2)_{14}\text{COOSi}(\text{CH}_3)_2]^+$ , Fig. S5) and 329 ( $[\text{CH}_3(\text{CH}_2)_{14}\text{C}(\text{OSi}(\text{CH}_3)_3)\text{OH}]^+$ , Fig. S5) suggesting a  $C_{16}$  acid ester containing a (TMS-derivatized) hydroxyl function in its alkyl moiety (Rontani and Aubert, 2004).

Considering all the MS evidence thus far, the compounds in **B** were surmised to be fatty acid esters of alkanediols and hence positional isomers of the compounds in series **A**. In accordance with this, the two most abundant fragments in the spectrum of each (TMS-derivatized) compound in **B** could be interpreted as  $\alpha$ -fragments generated on either side of the secondary hydroxyl group located in the alkyl chain of a wax ester. For example, the fragments  $m/z$  441 and 425 (for the homolog eluting at ca. 54 min) were explained as  $[\text{CH}_3(\text{CH}_2)_{22}\text{CHOSi}(\text{CH}_3)_3]^+$  and  $[\text{CH}_3(\text{CH}_2)_{14}\text{COO}(\text{CH}_2)_6\text{CHOSi}(\text{CH}_3)_3]^+$ , respectively, and therefore pointed to a 1,7-constellation of one primary and one secondary

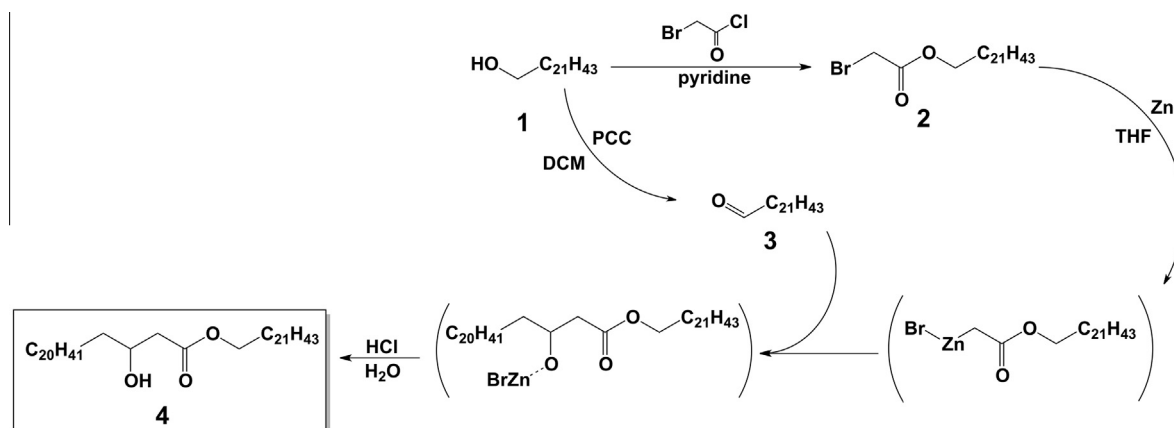


**Fig. 2.** Synthesis of a  $C_{46}$   $\beta$ -hydroxy fatty acid ester (docosyl 3-hydroxytetracosanoate). Docosanol (**1**) was converted into docosanal (**3**) as well as bromoacetate ester **2** and the corresponding organo-zinc reagent, which was then combined with **3** to form docosyl 3-hydroxytetracosanoate (**4**). Compounds in parentheses were not isolated, but used directly in the following step. Yields and procedural details are in the Experimental section. Abbreviations: PCC = pyridinium chlorochromate, DCM = dichloromethane, THF = tetrahydrofuran.

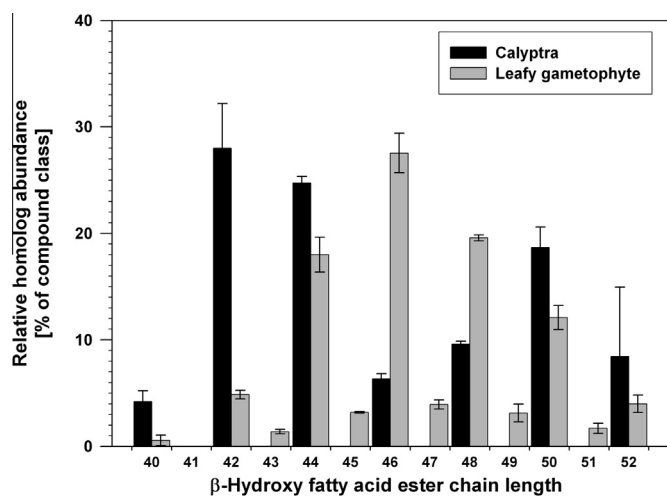


**Fig. 3.** Quantification of hydroxy ester homologs in *Funaria hygrometrica* waxes. Relative abundances of homologous  $\beta$ -hydroxy fatty acid esters on the calyptra (black) and leafy gametophyte (grey) were determined by integrating selected ion chromatograms ( $m/z$  161). Values are means of three independent parallels, with error bars indicating standard deviation.

hydroxyl function in the alkyl moiety of the ester (Fig. 4E). Satellite fragments of each of these  $\alpha$ -fragments were present in the spectrum from each homolog ( $m/z$  413 and 469, as well as  $m/z$  397 and 453, respectively, for the homolog shown in Fig. 4C). These could be explained as  $\alpha$ -fragments from co-eluting isomers in which the hydroxyl group was five or nine carbons away from the ester group. With all major fragments in the spectra thus explained, compounds in **B** were tentatively assigned to a homologous series of 1,X-diol ester isomers ( $X = 5, 7, \text{ or } 9$ ).

In order to confirm the 1,X-diol ester structure of compounds in **B**, the synthesis of a representative of this compound class was attempted. Considering the two functional groups in the target molecule, a synthetic scheme was designed where the secondary hydroxyl functionality was generated first, via Grignard reaction, and the ester group second, using an acyl chloride (Fig. 5). One hydroxyl group of 1,6-hexanediol (**5**) was substituted with bromine (**6**), the other protected as a tetrahydropyranyl ether, and then the resulting compound (**7**) was added to magnesium to afford the Grignard reagent **7a**. In parallel, tetracosanoic acid (**8**) was converted in two redox steps via the corresponding alcohol

(**9**) into tetracosanal (**10**). Finally, **7a** and **10** were combined to afford 1,7-triacontanediol (**11**). Information regarding mass and  $^1\text{H}$  NMR spectroscopic characterization of the intermediates in this synthesis is provided in the Supplementary data (Figs. S6 and S7).

An aliquot of **11** was further reacted with 4-dimethylaminopyridine (DMAP) and palmitoyl chloride to produce the target compound **12**. Selective acylation of the primary hydroxyl group was achieved by using limiting amounts of DMAP and palmitoyl chloride. The diol ester product of this reaction was purified by TLC, transformed into the corresponding TMS derivative, and characterized by GC–MS. Both the retention behavior and MS characteristics of **12** matched those of one isomer in the middle homolog of series **B** (Fig. 4A–D). This match of properties thus confirmed the 1,X-diol ester structure of one major compound in **B**. Interestingly, closer inspection established that the tetracosanoic acid starting material for synthesis of **12** contained a minor impurity in the form of docosanoic acid, which resulted in small amounts of homolog byproducts in all steps and finally led to 7-hydroxyoctacosyl palmitate observed as a small peak in the selected ion chromatogram of the synthetic product (Fig. 4B). The mass spectrum of its TMS derivative showed all the characteristics expected according to the above interpretation of diol ester MS fragmentations, thus providing further support for the homologous nature of the series.

Overall, a series of 1,X-diol esters with even-numbered chain lengths  $C_{40}$ – $C_{52}$  and odd-numbered homologs  $C_{45}$  and  $C_{47}$  was identified (Fig. 4A). The abundance of the satellite  $\alpha$ -fragments described above was used to determine the approximate ratio of esterified 1,5-, 1,7-, and 1,9-diol isomers (secondary hydroxyl position isomers) to be 1:4:1, which was roughly the same for all homologs. Finally, the relative amount of each diol ester homolog was quantified by integrating the selected ion chromatogram for  $m/z$  425 (Fig. 4A). Their distribution was approximately normal and the  $C_{46}$  homolog had the highest abundance (Fig. 6).

### 2.3. Identification of other bifunctional wax components

By detailed examination of the GC–MS traces, two diols were also identified in the wax from *F. hygrometrica*. First, in the calyptra and leafy gametophyte waxes, 1,3-octacosanediol was found based on previous reports of  $C_{22}$  and  $C_{26}$  VLC 1,3-diols (Vermeer et al., 2003; Buschhaus et al., 2013). The mass spectrum of this compound displayed characteristic  $\alpha$ -fragments and peaks at  $m/z$  73 ( $[\text{Si}(\text{CH}_3)_3]^+$ ), 103 ( $[\text{CH}_2\text{OSi}(\text{CH}_3)_3]^+$ ), and 147 ( $[(\text{CH}_3)_3\text{SiOSi}(\text{CH}_3)_2]^+$ ) (Fig. S8). Second, 1,7-triacontanediol (**11**) was identified

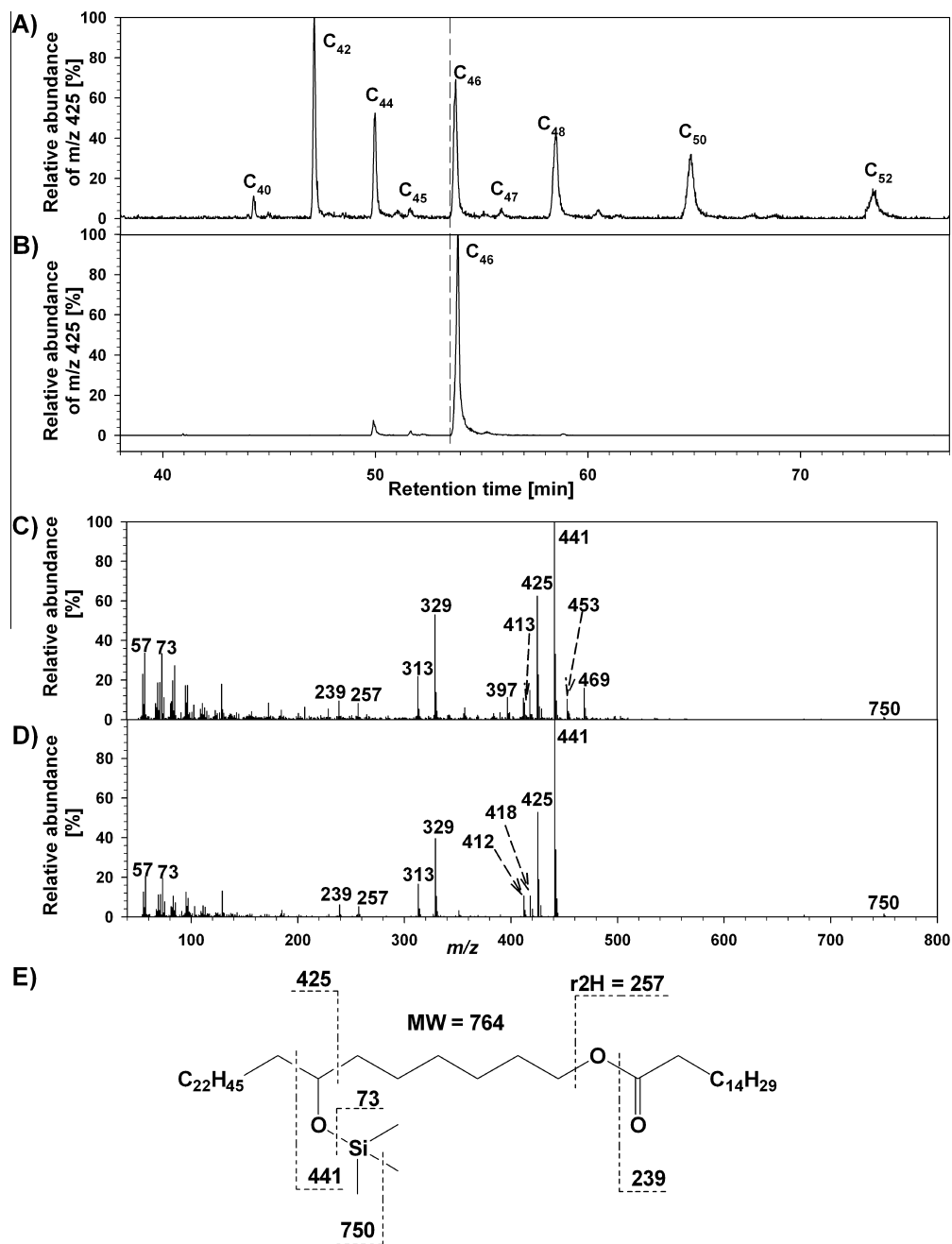


**Fig. 4.** Identification of unknown series **B** found in *Funaria hygrometrica* sporophyte capsule wax. (A) Selected ion chromatogram ( $m/z$  425) of the total wax mixture extracted from the capsules, depicting homologous series **B**. (B) Selected ion chromatogram ( $m/z$  425) of the synthetic  $C_{46}$  1,7-diol ester (7-hydroxytriacontyl palmitate (**12**), obtained from 1,6-hexane diol (**5**), see Fig. 5). (C) EI mass spectrum of the  $C_{46}$  homolog of series **B**. (D) EI mass spectrum of the synthetic  $C_{46}$  1,7-diol ester shown in (B). (E) Potential routes to the major fragments observed in the mass spectra of the  $C_{46}$  1,7-diol ester. Additional fragmentation mechanisms and ions resulting from the fragmentation of other  $C_{46}$  1,X-diol ester isomers are described in Fig. S6.

in the wax of the sporophyte capsule. Its mass spectrum also contained fragments with  $m/z$  73, 103, and 147, characteristic  $\alpha$ -fragments, a peak at  $m/z$  584 ( $[M-CH_3]^+$ ), and the products of single elimination of  $[HOSi(CH_3)_3]$  from both the intact molecule (giving rise to  $[CH_3(CH_2)_{22}CHOSi(CH_3)_3(CH_2)_4CHCH_2]^+$ ,  $m/z$  509) and the bifunctional  $\alpha$ -fragment (observed as  $[CHOSi(CH_3)_3(CH_2)_4CHCH_2]^+$ ,  $m/z$  185). Confirmation of this structural assignment was provided by a 1,7-triacontanediol standard (Fig. S9), obtained as an intermediate in the synthesis of 7-hydroxytriacontyl palmitate. Further searches using similar strategies failed to provide evidence for the presence of other 1,X-diols.

Finally, the wax mixtures from the leafy gametophyte and calyptra were searched for traces of the  $\beta$ -hydroxy acid esters, and the sporophyte capsule wax for the 1,X-diol esters. No evidence was found for presence of the novel compounds outside the moss structures where they had originally been identified. Also absent from all the wax samples was any indication of structural variants of series **B**, for example, a diol ester in which the secondary hydroxyl group was esterified instead of the terminal hydroxyl group. The possibility of bis-esterified 1,X-diol esters (where both the terminal and midchain hydroxyl groups had been esterified with a fatty acid) cannot be excluded because it is likely

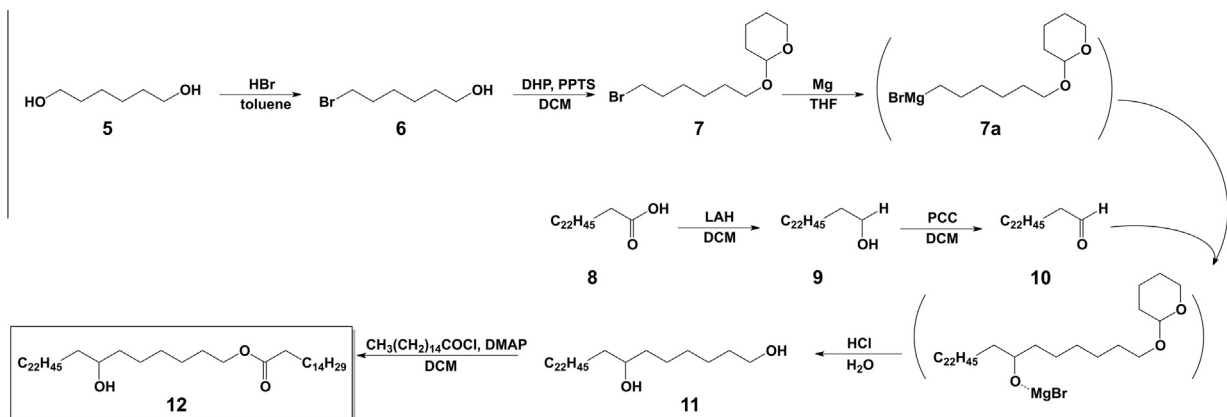


**Fig. 5.** Synthesis of 7-hydroxytriacontyl palmitate. Tetracosanal (**10**), as obtained from tetracosanoic acid through two redox steps, was added to the Grignard reagent **7a** obtained from THP-protected, brominated 1,6-hexanediol (**5**). An acidic workup afforded 1,7-triacontanediol (**11**), which was then esterified with palmitoyl chloride to form 7-hydroxytriacontyl palmitate (**12**). Compounds in parentheses were not isolated, but used directly in the following step. Yields and procedural details are given in the Experimental section. Abbreviations: LAH = lithium aluminum hydride, DMAP = 4-dimethylaminopyridine.

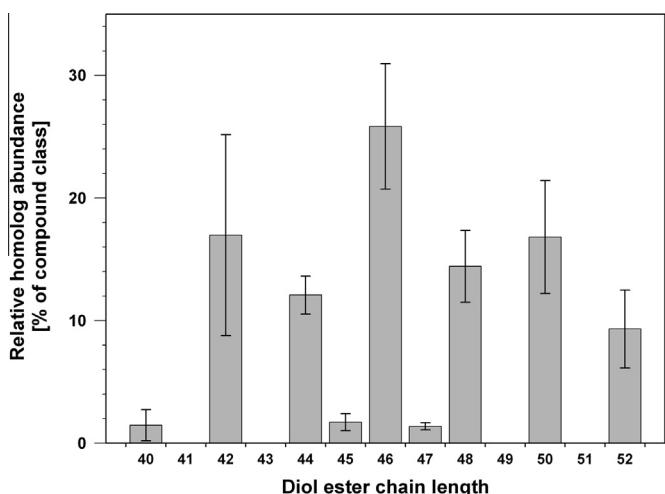


**Fig. 6.** Relative abundances of homologous diol esters in *Funaria hygrometrica* sporophyte capsule wax. Amounts are reported as the average of  $n = 3$  replicate samples quantified by integrating the selected ion chromatograms ( $m/z$  425). Error bars denote standard deviation.

that these molecules would escape detection, as they would be too large to elute from the GC within the 77-min run time programmed here.

### 3. Discussion

This report presents the structure elucidation of two novel classes of wax compounds from three surfaces of the moss *F. hygrometrica*. Waxes from the leafy gametophyte and calyptra contained  $\beta$ -hydroxy fatty acid esters, while those on the sporophyte capsule comprised 1,X-alkanediol esters instead. Both compound classes had several structural features in common, including the ester linkage between two unbranched, fully saturated hydrocarbon chains bearing terminal carboxyl or hydroxyl groups. Most notably, all the ester structures further contained one additional secondary hydroxyl function, albeit in varying positions. Overall, both compound classes may thus be described as ester-linked dimers of one mono- and one bifunctional VLC compound.

While wax constituents with primary functionality typically occur in simple homologous series, those with secondary groups frequently exhibit additional regio-isomerism. Accordingly, the bifunctional monomers contained within the two ester classes,

combining a primary and a secondary functional group, had the potential for homology as well as isomerism. Interestingly, only a few characteristic homologs and isomers were found for each bifunctional ester monomer, all of them with a secondary hydroxyl group, an odd number of methylene units between the primary and secondary functionalities, and predominantly even-numbered overall carbon chain length. Both types of bifunctional monomers hence had a strict 1,X-constellation of functionalities, where X was an odd number. These commonalities indicate that both bifunctional monomers co-occurring in the same plant species may be biosynthetically related and, based on the specific isomer and homolog distributions, that their common biosynthetic pathway may be hypothesized. This should aid and enable future biochemical investigations into the machinery involved in the production of these specialty compounds. Towards this end, discussed here are possible reaction steps leading to  $\beta$ -hydroxy fatty acid esters and alkanediol esters.

#### 3.1. Potential pathway leading to $\beta$ -hydroxy fatty acid esters

The *F. hygrometrica*  $\beta$ -hydroxy fatty acid esters had predominantly even-numbered total carbon chain lengths ranging from C<sub>40</sub> to C<sub>52</sub>, resulting from combination of acyl and alkyl portions each between 20 and 26 carbons in length. Furthermore, the additional secondary hydroxyl group was found exclusively on C-3 of the acyl moiety. These characteristics suggest that the  $\beta$ -hydroxy functionality is biosynthesized either by introducing the hydroxyl group into a pre-existing fatty acyl chain or as a by-product of chain elongation.

Two scenarios may be distinguished for introduction of a hydroxyl group into a pre-existing fatty acyl chain. In one, free or esterified acyl chains may be hydroxylated by a P450-dependent enzyme similar to the Arabidopsis mid-chain alkane hydroxylase (MAH1). However, MAH1 has only limited regioselectivity, repeatedly oxidizing up to three adjacent methylene units (Greer et al., 2007; Wen and Jetter, 2009). Therefore, a P450 enzyme clearly distinct from MAH1 would have to be invoked for formation of the strict 1,3-geometry of functional groups observed in the *F. hygrometrica*  $\beta$ -hydroxy fatty acid esters. Alternatively, the 3-hydroxyl group might also stem from mitochondrial fatty acid  $\beta$ -oxidation. While this would explain the specific location of the functional group, it would likely necessitate transport of intermediates from mitochondria to the endoplasmic reticulum as the compartment for wax ester biosynthesis and origin of wax export (Bernard and

Joubès, 2013). Neither of the two scenarios involving hydroxylation of a pre-existing fatty acyl chain is able to account for the chain length distribution of the *F. hygrometrica*  $\beta$ -hydroxyacyls.

To better explain the homolog specificity of  $\beta$ -hydroxyacyl formation, two more scenarios can be envisioned, with introduction of the hydroxyl group as a by-product of chain elongation. For one, a polyketide synthase (PKS) enzyme could use VLC acyl-CoAs as starters for condensation with one  $C_2$  unit from a malonyl-CoA to form  $\beta$ -ketoacyls. Most plant PKSs use aromatic starters, but some have been shown to also accept aliphatic substrates, albeit usually for multiple condensation rounds. Accordingly, PKSs have been invoked in biosynthesis of certain wax constituents in other plant species, mostly to form  $\beta$ -keto compounds (von Wettstein-Knowles, 1995), and thus a *F. hygrometrica* PKS generating VLC  $\beta$ -ketoacyls may be hypothesized. However, it would likely have to be associated with a reductase to transform the ketoacyls into the corresponding  $\beta$ -hydroxy compounds. There is no precedence for a PKS/reductase complex with activity towards VLC substrates.

Finally, the  $\beta$ -hydroxyacyl compounds could be diverted from normal wax biosynthesis, where they would occur as intermediates during fatty acid elongation. In the fatty acid elongase (FAE) complex, a KCS and KCR generate a  $\beta$ -hydroxyacyl intermediate that is usually channeled to the dehydratase and ECR components of the complex for transformation into the elongated acyl-CoA (Haslam and Kunst, 2013). However, it is feasible that the  $\beta$ -hydroxyacyl intermediate may be either released from the FAE complex or actively intercepted by an additional enzyme. A specific thioesterase intercepting intermediates between the KCR and the dehydratase of the FAE may be implicated in formation of the *F. hygrometrica*  $\beta$ -hydroxyacyls. Precedence exists for similar thioesterases, however with specificity for  $\beta$ -keto intermediates (intercepted after condensation rather than reduction) of medium-chain fatty acyl-ACPs (of the fatty acid synthase complex rather than the FAE) during the biosynthesis of methyl ketones in tomato (Yu et al., 2010).

The predominance of the  $C_{24}$   $\beta$ -hydroxy fatty acyl moiety in the *F. hygrometrica* esters suggests that potential intercept/release from the FAE might occur mainly during the elongation round from  $C_{22}$  to  $C_{24}$  acyl-CoA (Fig. 7, first dashed arrow). The presence of the other less abundant  $\beta$ -hydroxyacyl chain lengths in the ester products may then be explained by intercept/release occurring to a lesser extent during the adjacent rounds of elongation, i.e. those that produce  $C_{22}$  and  $C_{26}$  compounds. Most interestingly, the current results on homolog distribution of *F. hygrometrica*  $\beta$ -hydroxyacyls match those of previous reports on 1,3-bifunctional wax compounds in diverse higher plants. For example,  $C_{24}$  and  $C_{26}$  1,3-diols and hydroxyaldehydes were found in *Ricinus communis* (Vermeer et al., 2003),  $C_{22}$  and  $C_{24}$  1,3-diols have been identified in *Papaver orientale* (Jetter et al., 1996), and  $C_{20}$ ,  $C_{22}$  and  $C_{24}$  1,3-diols (accompanied by 1,2-diols) in *Cosmos bipinnatus* (Buschhaus et al., 2013). Overall, this points to the importance of the elongation round from  $C_{22}$  to  $C_{24}$  acyl-CoAs for the formation of 1,3 bifunctional compounds. However, a recent study showed similar  $\beta$ -hydroxy fatty acyl products in the wax of *A. arborescens*, but with chain lengths around  $C_{28}$ , and therefore thought to arise during elongation from  $C_{26}$  to  $C_{28}$  acyl-CoA (Racovita et al., 2014).

In contrast with previously characterized 1,3-bifunctional wax compounds, those of *F. hygrometrica* were esterified, suggesting involvement of a wax ester synthase similar to those involved in formation of esters lacking secondary hydroxyl functions. It is well established that these enzymes use fatty acyl-CoAs rather than free acids as substrates (Li et al., 2008). Consequently, a free  $\beta$ -hydroxy fatty acid generated by a thioesterase upon interception at the FAE would have to be re-activated into the CoA ester, likely by the action of a long-chain acyl-CoA synthase (LACS) enzyme. Alternatively, a passively released  $\beta$ -hydroxyacyl-CoA might be immediately available for esterification. In this context, it should

be noted that no free  $\beta$ -hydroxy fatty acids were found in the waxes from various moss surfaces investigated here, however this cannot be interpreted as evidence for either intermediate interception or release.

While VLC  $\beta$ -hydroxy fatty acid alkyl esters have not been previously identified in plants,  $C_{24}$ – $C_{32}$   $\beta$ -hydroxy fatty acid methyl esters were recently identified in *A. arborescens* cuticular waxes (Racovita et al., 2014). The hypothesized biosynthetic route to the acyl portion of these compounds was similar to that outlined above. However, the latter portion of biosynthesis is likely quite different between the methyl and alkyl esters. In the absence of methanol in biological contexts, methyl esters are typically formed by methylation of the carboxyl oxygen with *S*-adenosyl methionine (Dickschat et al., 2011; Nawrath et al., 2010). This is in contrast with the known biosynthesis of VLC alkyl esters, and likely by extension  $\beta$ -hydroxy acid esters, which occurs via acyl transfer onto a hydroxyl oxygen.

### 3.2. Potential pathway leading to 1,X-alkanediol esters

The second series of *F. hygrometrica* wax esters contained characteristic 1,X-alkanediols. When compared with the  $\beta$ -hydroxyacyl monomers, these diol monomers had a larger number of methylene units between the two functional groups (1,5-, 1,7-, and 1,9-geometry), longer overall chain lengths (mostly  $C_{30}$ ) and a hydroxyl as terminal functional group. Relatively little chain length and isomer variation was observed in the diol moieties of the esters, with  $C_{30}$  1,7-diol largely dominating. Thus, the chain length of the acyl portion was the sole determining factor of the total ester chain length, which ranged from  $C_{40}$  to  $C_{52}$  and was strongly dominated by even-numbered homologs.

The secondary hydroxyl function of the 1,X-alkanediols could be generated through P450 hydroxylase activity,  $\beta$ -oxidation, PKS-based elongation, or FAE intermediate intercept/release, similar to the mechanisms discussed above for  $\beta$ -hydroxyacyls. However, regioselectivity and literature precedence again favor a biosynthetic sequence that begins with intercept/release of a  $\beta$ -hydroxyacyl intermediate of elongation by the FAE complex. The two pathways to VLC diol esters and  $\beta$ -hydroxy fatty acid esters thus could share the  $\beta$ -hydroxyacyl-CoA (and/or free  $\beta$ -hydroxy fatty acids) as intermediate(s), but they diverge beyond this point (Fig. 7). While  $\beta$ -hydroxy fatty acid ester biosynthesis might require only one more step (acyl transfer), the hypothesized pathway to diol esters is more involved.

Formation of the predominant  $C_{30}$  1,7-diol structure may be explained by intercept/release of the  $\beta$ -hydroxyacyl intermediate of the elongation round leading from  $C_{24}$  to  $C_{26}$  acyl-CoA. The resulting  $C_{26}$   $\beta$ -hydroxyacyl-CoA could then re-enter an FAE for two more elongation rounds to yield  $C_{30}$  7-hydroxyacyl-CoA (Fig. 7, bold arrows). Similarly, other  $\beta$ -hydroxyacyl intermediates might be intercepted in the elongation rounds leading to  $C_{28}$  and  $C_{24}$  acyl-CoA, which upon being elongated by one or three rounds, respectively, would generate  $C_{30}$  5- and 9-hydroxyacyl-CoAs.

The co-occurrence of esterified and free 1,X-alkanediols in the same moss structures strongly suggests that both compound classes are biosynthetically related, most likely with the free diols serving as precursors for esterification. This implies that the 5-, 7-, and 9-hydroxyacyl-CoA intermediates first have their carboxyl head groups reduced, leading to 1,5-, 1,7-, and 1,9- $C_{30}$  diols, respectively. Such a reduction could potentially be accomplished by a fatty acyl reductase (FAR) enzyme similar to those involved in acyl reduction to ubiquitous wax alkanols. The resulting free 1,5-, 1,7-, and 1,9-diols could then be exported to the cuticle, or could be available for esterification. It should be noted that similar free 1,7-diols had been described as cuticular wax components in various *Papaver* species (Jetter and Riederer, 1996), in homolog

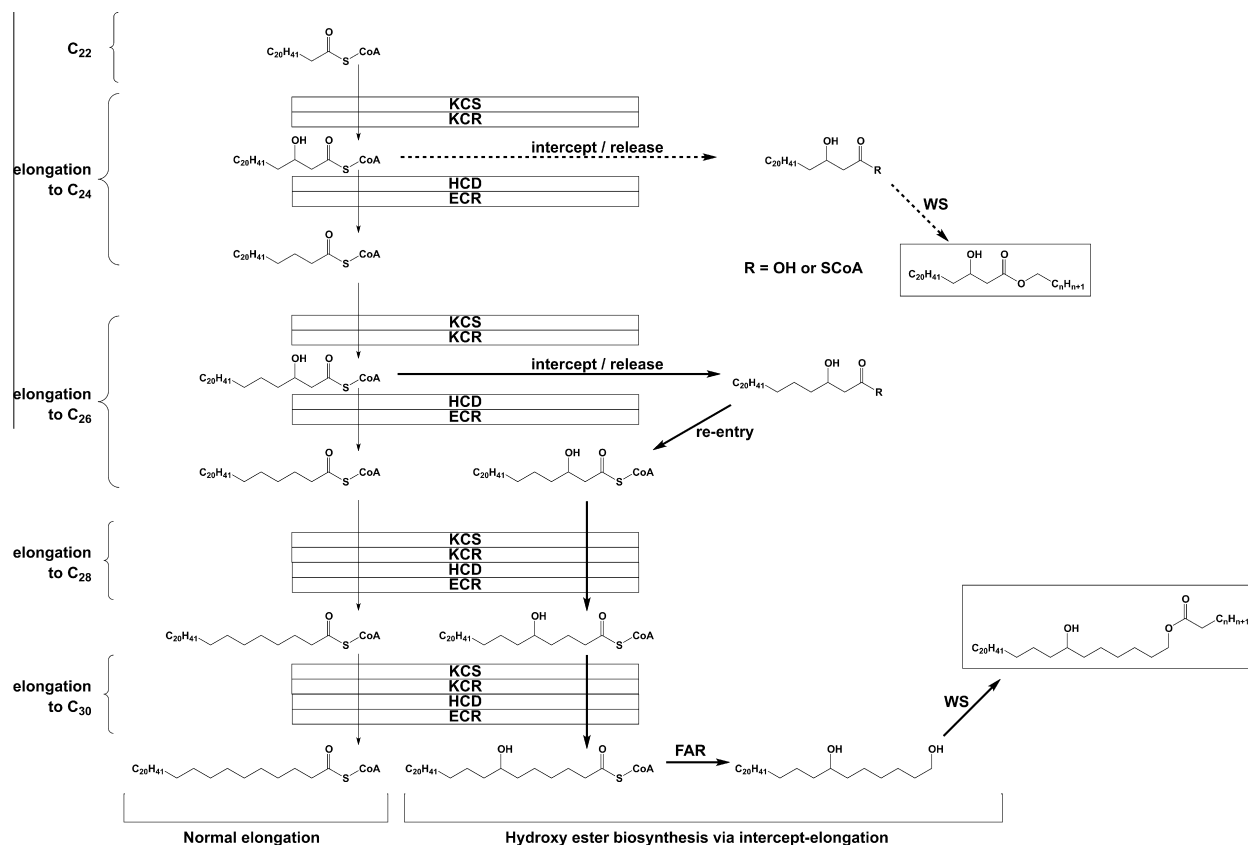


**Fig. 7.** Biosynthesis model for the hydroxy esters found in *Funaria hygrometrica* waxes. Normal arrows indicate reactions in the biosynthesis of normal very-long-chain fatty acid elongation. Dotted arrows indicate the hypothesized pathway to  $\beta$ -hydroxy fatty acid esters via a wax ester synthase (WS). Bold arrows indicate the proposed biosynthesis of the 1,7-diol esters via a fatty acyl reductase (FAR) and WS. Elongation is carried out by four enzymes, the names of which have been abbreviated: ketoacyl-CoA synthase (KCS), ketoacyl-CoA reductase (KCR), hydroxyacyl-CoA dehydratase (HCD), and enoyl-CoA reductase (ECR).

and isomer mixtures similar to those found for *F. hygrometrica*, albeit in free (not esterified) form. Other 1,X-diols have been reported from the fern *Azolla filliculoides* and several algae species, though were found as 1,13- through 1,19-diols (inclusive) (Méjanelle et al., 2003; Speelman et al., 2009; Volkman et al., 1999), indicating that the biosynthesis of these compounds may be different from the products described here.

While a fraction of the *F. hygrometrica* 1,X-alkanediols are exported to the cuticle without further modification, the majority were observed to be esterified with VLC acids. It seems likely that the necessary acyl transfer may be catalyzed by a wax ester synthase similar to those involved in normal wax ester biosynthesis above. Similar diol esters have been found, for example, in the stem bark of *Tectona grandis* as a mixture of 7-hydroxyoctacosyl decanoate, 18-hydroxyhexacosyl decanoate, and 20-hydroxyeicosyl linolenate (Khan et al., 2010), in *A. filliculoides* ferns as 1,13-, 1,15-, and 1,17-alkanediol  $C_{48}$  esters (Speelman et al., 2009), and in *Laurus nobilis* fruits as a 1,19-alkanediol  $C_{42}$  ester (Garg et al., 1992). Pea weevil insects also produce a VLC diol ester (22-hydroxydocosyl hydroxypropanoate) that serves as a mitogen (Oliver et al., 2000). Finally, esters of  $C_{30}$  and  $C_{32}$  1,11- and 1,13-hydroxyketones have been identified in wax from *O. regalis* fronds (Jetter and Riederer, 1999b). Nevertheless, VLC 1,X-alkanediol esters have not been described before as components of cuticular waxes.

#### 4. Conclusions

In summary, two novel compound classes were identified in the waxes of the moss *F. hygrometrica*, both with characteristic

homolog and isomer patterns. Based on their common chemical features, it is proposed that the bifunctional monomers originate through intercept and/or release of  $\beta$ -hydroxyacyl intermediates of the FAE complex followed by further modification. On one hand, the  $\beta$ -hydroxyacyl-CoA intermediates from the FAE may be esterified with wax alkanols, or they may re-enter into the FAE cycle following which subsequent FAR reduction may lead to 1,5-, 1,7-, and 1,9-diols. These may then be esterified with fatty acids (Fig. 7). The shared biosynthetic elements may be fine-tuned in each moss structure to generate the respective isomer and homolog distributions of the compounds identified.

The proposed biosynthetic pathways explain the observed similarities and differences between the two novel natural product classes and require very few new or modified enzymatic steps. It seems plausible that either a special FAE allowing release of  $\beta$ -hydroxyacyls or recruitment of a thioesterase could generate the necessary precursors. Furthermore, slight modifications in the substrate specificities of certain known wax biosynthetic enzymes could then account for the biosynthesis of the distinct homolog distributions of these two major classes of wax compounds in the moss. However, it should be emphasized that, based on the current chemical data alone, these biosynthetic pathways can be tentatively laid out but not proven. Important questions arising from this discussion include the involvement of a thioesterase interacting with (one of) the FAE complex(es) in *F. hygrometrica*, and the alternative pathways invoking PKS or P450 enzymes for the formation of secondary functional groups in the 1,X-bifunctional compounds found here. Together, the implied models present directions for future research.

## 5. Experimental

### 5.1. Growth conditions, wax extraction, purification, and transesterification

Collections of *F. hygrometrica* were made from four Connecticut populations with developing sporophytes (CONN – Budke #142, #144, #145; Goffinet #9027). Spores from several sporophytes per site were used to establish laboratory populations for each locality. Laboratory populations were grown, cold treated to stimulate reproduction, and further cultivated to produce sporophytes as described previously (Budke et al., 2011).

Each wax sample contained the cuticular wax from twenty square centimeters of plant surface area (74 leafy gametophytes, 465 calyptrae, or 235 sporophyte capsules). Three samples of each moss structure's cuticular wax were prepared. To create a sample, each structure was chemically extracted by rinsing in  $\text{CHCl}_3$  (4 mL  $\times$  2) (Aldrich), for 30 s each time. Cut ends of sporophyte capsules and leafy gametophytes were held out of the  $\text{CHCl}_3$  to avoid extraction of internal lipids. The extracts from both rinses were pooled and filtered, and *n*-tetracosane was added as an internal standard. The  $\text{CHCl}_3$  was evaporated by air-drying overnight prior to analysis.

Isolation of individual compound classes, where necessary and/or possible, was accomplished by loading a wax extract or reaction mixture onto a TLC plate of 0.25 mm thickness (Analtech), which was then developed with  $\text{CHCl}_3$ :EtOH (99:1). The plates were stained with primuline (Aldrich) dissolved in acetone, and bands were visualized under UV light (365 nm). Bands were excised, adsorbed compounds extracted from silica using  $\text{CHCl}_3$ , and the solvent evaporated. Transesterification of resulting mixtures was carried out by dissolving in 14%  $\text{BF}_3$  in MeOH (100  $\mu\text{l}$ ) (Aldrich), incubating at 70 °C for 18 h, then evaporating excess reagent under a stream of  $\text{N}_2$ .

### 5.2. Derivatization and GC–MS analysis

Derivatization was accomplished by dissolving each sample in 10  $\mu\text{l}$  of both pyridine (Aldrich) and BSTFA (Aldrich), reacting at 70 °C for 45 min, evaporating excess reagents at 60 °C under a stream of  $\text{N}_2$ , and finally dissolving in  $\text{CHCl}_3$  (10  $\mu\text{l}$ ).

Wax analyses were carried out on a 6890 N Network GC (Agilent) equipped with an HP-1 capillary column (Agilent, length 30 m, i.d. 320  $\mu\text{m}$ , 1  $\mu\text{m}$  film thickness). 1  $\mu\text{l}$  of each sample was injected on-column into a flow of He programmed for constant flow at 1.4 ml/min. The GC oven was held at 50 °C for 2 min, followed by a 40 °C/min ramp to 200 °C, held at 200 °C for 2 min, increased by 3 °C/min to 320 °C, and held at 320 °C for 30 min. Analytes were detected with an Agilent 5793N Mass Selective Detector (EI 70 eV; *m/z* 50–800, 1 scan  $\text{s}^{-1}$ ).

### 5.3. Synthesis of authentic standards

Dry solvents, when required, were dried over activated molecular sieves for 24 h. Other materials were used as received from the supplier. Column chromatography (CC) was performed using Silicycle SilicaFlash G60 (60–200  $\mu\text{m}$  size, 70–230 mesh).  $^1\text{H}$  NMR spectra were obtained using a Bruker Avance 300 MHz NMR spectrometer ( $\text{CDCl}_3$ , 25 °C). TLC comparison of synthetic and biological compounds was performed using analytical silica gel 60 TLC plates on aluminum (Merck) developed in  $\text{CHCl}_3$ :EtOH (99:1).

#### 5.3.1. Docosyl 2-bromoacetate (**2**)

Docosanol (200 mg, 1 eq.) was dissolved in dry  $\text{CH}_2\text{Cl}_2$ , then bromoacetyl chloride (113 mg, 60  $\mu\text{l}$ , 1.2 eq.) and pyridine (30  $\mu\text{l}$ ,

0.6 eq.) were added. When TLC (developed in toluene) indicated alcohol consumption, the reaction was washed with HCl (1 M), and the mixture was loaded onto a silica column. Eluting with hexane:toluene (2:1) yielded docosyl 2-bromoacetate, which was used in the next step without further purification (50 mg, 20% crude yield).

#### 5.3.2. Docosanal (**3**)

Docosanol (200 mg, 1 eq.) was dissolved in dry  $\text{CH}_2\text{Cl}_2$  (20 ml), and PCC (130 mg, 1 eq.) was added. The mixture was stirred at room temperature overnight, after which the solvent was evaporated, the remaining solid dissolved in hexane: $\text{CHCl}_3$  (2 ml, 1:1) and purified by CC using hexane: $\text{CHCl}_3$  (1:1) to afford docosanal (139 mg, 70% yield).

#### 5.3.3. Docosyl 3-hydroxytetracosanoate (**4**)

Docosyl 2-bromoacetate (50 mg, **2**, 1 eq.), docosanal (29 mg, **3**, 0.7 eq.), zinc powder (13 mg, 1.5 eq.), and a small chip of iodine were dissolved in dry THF (20 ml). Heating was carried out until reflux began and the temperature was held overnight at 70 °C. When the consumption of the aldehyde was confirmed by TLC (developed in toluene) the reaction mixture was washed with HCl (1 M) and extracted with  $\text{Et}_2\text{O}$  ( $\times$ 3). The combined extracts were concentrated and loaded onto a preparative TLC plate alongside a small amount of unknown series **B** as purified from the leafy gametophyte wax extract. The plate was developed in toluene and stained with primuline. One band from the reaction mixture comigrated with the natural product, which was then excised and the  $\text{CHCl}_3$  extract was analyzed with GC–MS. Yield was not recorded.

#### 5.3.4. 1-Bromohexanol (**6**)

To a stirred solution of 1,6-hexanediol (6.0 g, 1 eq.) in toluene, HBr (7 ml, 9 M, 1.3 eq.) was added and allowed to react at 80 °C for 20 h. Then the reaction mixture was extracted with  $\text{Et}_2\text{O}$  ( $\times$ 3), the combined extracts dried over  $\text{Na}_2\text{SO}_4$ , filtered, and the solvent was removed under reduced pressure. The resulting liquid was purified by CC using hexane: $\text{Et}_2\text{O}$  (1:1) as mobile phase. From this, 1-bromohexanol was obtained (7.073 g, 73% yield).  $^1\text{H}$  NMR (300 MHz,  $\text{CDCl}_3$ ):  $\delta$  3.63 (2H, t, *J* = 6.6 Hz,  $\text{CH}_2\text{Br}$ ), 3.40 (2H, t, *J* = 6.6 Hz,  $\text{HOCH}_2$ ), 1.86 (2H, q, *J* = 7.2,  $\text{CH}_2\text{CH}_2\text{Br}$ ), 1.20–1.60 (6H, m, aliphatic **CH**).

#### 5.3.5. 2-((6-Bromohexyl)oxy)tetrahydro-2H-pyran (**7**)

1-Bromohexanol (7.0 g, 1 eq.) was dissolved in  $\text{CH}_2\text{Cl}_2$  and cooled with an ice bath, then dihydropyran (5.3 ml, 1.5 eq.) and pyridinium *p*-toluenesulfonate (50 mg, 0.05 eq.) were added. After stirring overnight, the mixture was washed with  $\text{H}_2\text{O}$  ( $\times$ 2), once with brine, dried with  $\text{Na}_2\text{SO}_4$ , filtered, and the solvent was removed under reduced pressure. The resulting solid was dissolved in hexane: $\text{Et}_2\text{O}$  (5 mL, 20:1), loaded onto a silica column, and eluted using hexane: $\text{Et}_2\text{O}$  (20:1). Product containing fractions were combined and the solvent removed to afford compound **7** (6.442 g, 61% yield).

#### 5.3.6. Tetracosanol (**9**)

A cold slurry of lithium aluminum hydride (LAH, 110 mg, 3 eq.) in THF under  $\text{N}_2$  was prepared. Tetracosanoic acid (400 mg, 1 eq.) was dissolved in dry THF and added dropwise to the slurry through a septum using a syringe. The reaction was stirred overnight at room temperature and then quenched with  $\text{H}_2\text{O}$ , the mixture was washed with dilute HCl and extracted with  $\text{Et}_2\text{O}$  ( $\times$ 3), the combined extracts were dried with  $\text{Na}_2\text{SO}_4$ , filtered, and the solvent was evaporated under reduced pressure. This afforded tetracosanol (0.3162 g, 82% yield).

### 5.3.7. Tetracosanal (10)

Tetracosanol (300 mg, **9**, 1 eq.) and pyridinium chlorochromate (215 mg, 1.3 eq.) were dissolved in 50 ml dry CH<sub>2</sub>Cl<sub>2</sub>. The mixture was gently heated until the solids dissolved and stirred overnight at room temperature. Then the solvent was removed under reduced pressure, the remaining solid was dissolved in CHCl<sub>3</sub> (5 ml), the solution was filtered through a short silica column, stirred with activated charcoal, and then filtered through another short silica column to yield tetracosanal (206 mg, 69% yield).

### 5.3.8. 1,7-Triacontanediol (11)

Mg powder (30 mg, 2 eq.) and a chip of iodine were suspended in dry THF (2 mL). Dry tetracosanal (200 mg, **10**, 1.3 eq.) and dry compound **7** (188 mg, 1 eq.) were each dissolved in dry THF (5 ml). Compound **7** was added dropwise at 70 °C and the mixture was refluxed for 3 h; **10** was then added dropwise and the reaction cooled and stirred overnight. The reaction was then quenched with H<sub>2</sub>O, the mixture acidified with HCl and extracted with Et<sub>2</sub>O (×3), the combined extracts washed with saturated NaCl, dried with Na<sub>2</sub>SO<sub>4</sub>, filtered, and the solvent evaporated under reduced pressure. A small portion of the resulting solid was loaded onto a TLC plate and developed with CHCl<sub>3</sub>, from which approximately 10 mg of the desired product, 1,7-triacontanediol, were recovered and analyzed with GC–MS. Yield was not recorded.

### 5.3.9. 7-Hydroxytriacontyl palmitate (12)

1,7-Triacontanediol (2 mg) was dissolved in dry CH<sub>2</sub>Cl<sub>2</sub> (50 μl), to which was added 4-dimethylaminopyridine (1 mg) and palmitoyl chloride (0.1 μl). After one hour stirring, the entire mixture was loaded onto an analytical TLC plate and developed in CHCl<sub>3</sub>:EtOH (99:1). GC–MS analysis of the three resulting bands revealed they contained palmitic acid, DMAP, and 7-hydroxytriacontyl palmitate. Yield was not recorded.

## Acknowledgments

The assistance of S. Komar and E. Magat with extraction of *F. hygrometrica* leafy gametophytes is recognized with appreciation, as is the technical assistance and advice of C. Peng on the diol ester synthesis. This work has been made possible by generous support from the Natural Sciences and Engineering Research Council (Canada), the Canada Research Chairs Program, the Canada Foundation for Innovation, the US National Science Foundation (DEB-1146295), and a Katherine Esau Postdoctoral Fellowship to J.M.B.

## Appendix A. Supplementary data

Supplementary data associated with this article can be found, in the online version, at <http://dx.doi.org/10.1016/j.phytochem.2015.10.007>.

## References

- Bach, L., Michaelson, L.V., Haslam, R., Bellec, Y., Gissot, L., Marion, J., Da Costa, M., Boutin, J.-P., Miquel, M., Tellier, F., Domergue, F., Markham, J.E., Beaudoin, F., Napier, J.A., Faure, J.-D., 2008. The very-long-chain hydroxy fatty acyl-CoA dehydratase PASTICCINO2 is essential and limiting for plant development. *Proc. Natl. Acad. Sci.* 105, 14727–14731.
- Barthlott, W., Neinhuis, C., Cutler, D., Ditsch, F., Meusel, I., Theisen, I., Wilhelm, H., 1998. Classification and terminology of plant epicuticular waxes. *Bot. J. Linn. Soc.* 126, 237–260.
- Barthlott, W., Neinhuis, C., Jetter, R., Bourauel, T., Riederer, M., 1996. Waterlily, poppy, or sycamore: on the systematic position of *Nelumbo*. *Flora* 191, 169–174.
- Beaudoin, F., Wu, X., Li, F., Haslam, R.P., Markham, J.E., Zheng, H., Napier, J.A., Kunst, L., 2009. Functional characterization of the *Arabidopsis* β-ketoacyl-coenzyme A reductase candidates of the fatty acid elongase. *Plant Physiol.* 150, 1174–1191.
- Bernard, A., Domergue, F., Pascal, S., Jetter, R., Renne, C., Faure, J.-D., Haslam, R.P., Napier, J.A., Lessire, R., Joubès, J., 2012. Reconstitution of plant alkane biosynthesis in yeast demonstrates that *Arabidopsis* ECERIFERUM1 and ECERIFERUM3 are core components of a very-long-chain alkane synthesis complex. *Plant Cell* 24, 1–14.
- Bernard, A., Joubès, J., 2013. *Arabidopsis* cuticular waxes: advances in synthesis, export and regulation. *Prog. Lipid Res.* 52, 110–129.
- Buda, G.J., Barnes, W.J., Fich, E.A., Park, S., Yeats, T.H., Zhao, L., Domozych, D.S., Rose, J.K.C., 2013. An ATP binding cassette transporter is required for cuticular wax deposition and desiccation tolerance in the moss *Physcomitrella patens*. *Plant Cell* 25, 4000–4013.
- Budke, J.M., Goffinet, B., Jones, C.S., 2011. A hundred-year-old question: is the moss calyptra covered by a cuticle? A case study of *Funaria hygrometrica*. *Ann. Bot.* 107, 1279–1286.
- Buschhaus, C., Peng, C., Jetter, R., 2013. Very-long-chain 1,2- and 1,3-bifunctional compounds from the cuticular wax of *Cosmos bipinnatus* petals. *Phytochemistry* 91, 249–256.
- Chen, X., Goodwin, S.M., Boroff, V.L., Liu, X., Jenks, M.A., 2003. Cloning and characterization of the WAX2 gene of *Arabidopsis* involved in cuticle membrane and wax production. *Plant Cell* 15, 1170–1185.
- Dickschat, J.S., Bruns, H., Riclea, R., 2011. Novel fatty acid methyl esters from the actinomycete *Micromonospora aurantiaca*. *Beilstein J. Org. Chem.* 7, 1697–1712.
- Dominguez, E., Heredia-Guerrero, J.A., Heredia, A., 2011. The biophysical design of plant cuticles: an overview. *New Phytol.* 189, 938–949.
- Garg, S.N., Siddiqui, M.S., Agarwal, S.K., 1992. New fatty acid esters and hydroxy ketones from the fruits of *Laurus nobilis*. *J. Nat. Prod.* 55, 1315–1319.
- Greer, S., Wen, M., Bird, D., Wu, X., Samuels, L., Kunst, L., Jetter, R., 2007. The cytochrome P450 enzyme CYP96A15 is the midchain alkane hydroxylase responsible for formation of secondary alcohols and ketones in stem cuticular wax of *Arabidopsis*. *Plant Physiol.* 145, 653–667.
- Haas, K., 1982. Surface wax of *Andraea* and *Pogonatum* species. *Phytochemistry* 21, 657–659.
- Haslam, T.M., Kunst, L., 2013. Extending the story of very-long-chain fatty acid elongation. *Plant Sci.* 210, 93–107.
- Jenks, M.A., Tuttle, H.A., Eigenbrode, S.D., Feldmann, K.A., 1995. Leaf epicuticular waxes of the *eceriferum* mutants in *Arabidopsis*. *Plant Physiol.* 108, 369–377.
- Jetter, R., Kunst, L., Samuels, A.L., 2006. Composition of plant cuticular waxes. In: Riederer, M., Mueller, C. (Eds.), *Biology of the Plant Cuticle*. Blackwell, Oxford, pp. 145–181.
- Jetter, R., Riederer, M., 2000. Composition of cuticular waxes on *Osmunda regalis* fronds. *J. Chem. Ecol.* 26, 399–412.
- Jetter, R., Riederer, M., 1999a. Homologous long-chain δ-lactones in leaf cuticular waxes of *Cerintho minor*. *Phytochemistry* 50, 1359–1364.
- Jetter, R., Riederer, M., 1999b. Long-chain alkanediols, ketoaldehydes, ketoalcohols and ketoalkyl esters in the cuticular waxes of *Osmunda regalis* fronds. *Phytochemistry* 52, 907–915.
- Jetter, R., Riederer, M., 1996. Cuticular waxes from the leaves and fruit capsules of eight Papaveraceae species. *Can. J. Bot.* 74, 419–430.
- Jetter, R., Riederer, M., Seyer, A., Mioskowski, C., 1996. Homologous long-chain alkanediols from *Papaver* leaf cuticular waxes. *Phytochemistry* 42, 1617–1620.
- Joubès, J., Raffaele, S., Bourdenx, B., Garcia, C., Laroche-Traineau, J., Moreau, P., Domergue, F., Lessire, R., 2008. The VLCFA elongase gene family in *Arabidopsis thaliana*: phylogenetic analysis, 3D modelling and expression profiling. *Plant Mol. Biol.* 67, 547–566.
- Khan, Z., Ali, M., Bagri, P., 2010. A new steroidal glycoside and fatty acid esters from the stem bark of *Tectona grandis* Linn. *Nat. Prod. Res.* 24, 1059–1068.
- Lai, C., Kunst, L., Jetter, R., 2007. Composition of alkyl esters in the cuticular wax on inflorescence stems of *Arabidopsis thaliana cer* mutants. *Plant J.* 50, 189–196.
- Lee, J., Yang, K., Lee, M., Kim, S., Kim, J., Lim, S., Kang, G.-H., Min, S.R., Kim, S.-J., Park, S.U., Jang, Y.S., Lim, S.S., Kim, H., 2015. Differentiated cuticular wax content and expression patterns of cuticular wax biosynthetic genes in bloomed and bloomless broccoli (*Brassica oleracea* var. *italica*). *Process Biochem.* 50, 456–462.
- Li, F., Wu, X., Lam, P., Bird, D., Zheng, H., Samuels, L., Jetter, R., Kunst, L., 2008. Identification of the wax ester synthase/acyl-coenzyme A: diacylglycerol acyltransferase WSD1 required for stem wax ester biosynthesis in *Arabidopsis*. *Plant Physiol.* 148, 97–107.
- Méjanelle, L., Sanchez-Gargallo, A., Bentaleb, I., Grimalt, J.O., 2003. Long chain n-alkyl diols, hydroxy ketones and sterols in a marine eustigmatophyte, *Nannochloropsis gaditana*, and in *Brachionus plicatilis* feeding on the algae. *Org. Geochem.* 34, 527–538.
- Nawrath, T., Gerth, K., Müller, R., Schulz, S., 2010. Volatile methyl esters of medium chain length from the bacterium *Chitinophaga Fx7914*. *Chem. Biodivers.* 7, 2228–2253.
- Neinhuis, C., Jetter, R., 1995. Epicuticular wax of Polytrichales sporophytes. *J. Bryol.* 18, 399–406.
- Oliver, J.E., Doss, R.P., Williamson, R.T., Carney, J.R., DeVilbiss, E.D., 2000. Bruchins—mitogenic 3-(hydroxypropanoyl) esters of long chain diols from weevils of the Bruchidae. *Tetrahedron* 56, 7633–7641.
- Racovita, R.C., Peng, C., Awakawa, T., Abe, I., Jetter, R., 2014. Very-long-chain 3-hydroxy fatty acids, 3-hydroxy fatty acid methyl esters and 2-alkanols from cuticular waxes of *Aloe arborescens* leaves. *Phytochemistry*, 1–12.
- Rashotte, A.M., Jenks, M.A., Feldmann, K.A., 2001. Cuticular waxes on *eceriferum* mutants of *Arabidopsis thaliana*. *Phytochemistry* 57, 115–123.
- Razeq, F.M., Kosma, D.K., Rowland, O., Molina, I., 2014. Extracellular lipids of *Camelina sativa*: characterization of chloroform-extractable waxes from aerial and subterranean surfaces. *Phytochemistry* 106, 188–196.
- Rontani, J.F., Aubert, C., 2004. Trimethylsilyl transfer during electron ionization mass spectral fragmentation of some ω-hydroxycarboxylic and ω-dicarboxylic

- acid trimethylsilyl derivatives and the effect of chain length. *Rapid Commun. Mass Spectrom.* 18, 1889–1895.
- Samuels, L., Kunst, L., Jetter, R., 2008. Sealing plant surfaces: cuticular wax formation by epidermal cells. *Annu. Rev. Plant Biol.* 59, 683–707.
- Speelman, E.N., Reichart, G.J., de Leeuw, J.W., Rijpstra, W.I.C., Sinnighe Damsté, J.S., 2009. Biomarker lipids of the freshwater fern *Azolla* and its fossil counterpart from the Eocene Arctic Ocean. *Org. Geochem.* 40, 628–637.
- Vermeer, C.P., Nastold, P., Jetter, R., 2003. Homologous very-long-chain 1,3-alkanediols and 3-hydroxyaldehydes in leaf cuticular waxes of *Ricinus communis* L. *Phytochemistry* 62, 433–438.
- Volkman, J.K., Barrett, S.M., Blackburn, S.I., 1999. Fatty acids and hydroxy fatty acids in three species of freshwater euglenophytes. *J. Phycol.* 35, 1005–1012.
- Von Wettstein-Knowles, P., 1995. Biosynthesis and genetics of waxes. In: Hamilton, R.J. (Ed.), *Waxes: Chemistry, Molecular Biology and Functions*. The Oily Press, Dundee, pp. 91–129.
- Von Wettstein-Knowles, P., 1993. Waxes, cutin, and suberin. In: Moore, T.S. (Ed.), *Lipid Metabolism in Plants*. CRC Press Inc, Boca Raton, pp. 127–166.
- Wen, M., Jetter, R., 2009. Composition of secondary alcohols, ketones, alkanediols, and ketols in *Arabidopsis thaliana* cuticular waxes. *J. Exp. Bot.* 60, 1811–1821.
- Wen, M., Jetter, R., 2007. Very-long-chain hydroxyaldehydes from the cuticular wax of *Taxus baccata* needles. *Phytochemistry* 68, 2563–2569.
- Xu, S.-J., Jiang, P.-A., Wang, Z.-W., Wang, Y., 2009. Crystal structures and chemical composition of leaf surface wax depositions on the desert moss *Syntrichia caninervis*. *Biochem. Syst. Ecol.* 37, 723–730.
- Yeats, T.H., Rose, J.K.C., 2013. The formation and function of plant cuticles. *Plant Physiol.* 163, 5–20.
- Yu, G., Nguyen, T.T.H., Guo, Y., Schauvinhold, I., Auldridge, M.E., Bhuiyan, N., Ben-Israel, I., Iijima, Y., Fridman, E., Noel, J.P., Pichersky, E., 2010. Enzymatic functions of wild tomato methylketone synthases 1 and 2. *Plant Physiol.* 154, 67–77.
- Zhang, X., Liu, Z., Wang, P., Wang, Q., Yang, S., Feng, H., 2013. Fine mapping of Br Wax1, a gene controlling cuticular wax biosynthesis in Chinese cabbage (*Brassica rapa* L. ssp. *pekinensis*). *Mol. Breed.* 32, 867–874.
- Zheng, H., Rowland, O., Kunst, L., 2005. Disruptions of the *Arabidopsis* enoyl-CoA reductase gene reveal an essential role for very-long-chain fatty acid synthesis in cell expansion during plant morphogenesis. *Am. Soc. Plant Biol.* 17, 1467–1481.